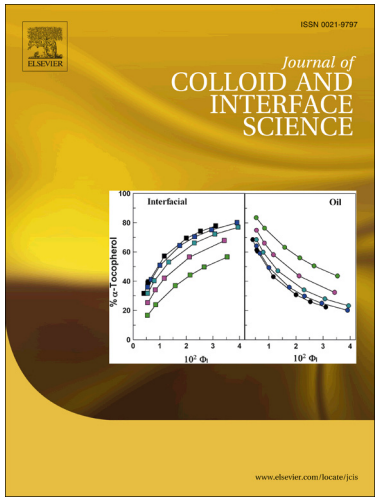

Synthesis of selenium particles with various morphologies

Ajeet Kumar, Igor Sevonkaev, Dan V. Goia

PII: S0021-9797(13)00953-3
DOI: http://dx.doi.org/10.1016/j.jcis.2013.10.046
Reference: YJCIS 19167

To appear in: *Journal of Colloid and Interface Science*

Received Date: 30 August 2013
Accepted Date: 21 October 2013

Please cite this article as: A. Kumar, I. Sevonkaev, D.V. Goia, Synthesis of selenium particles with various morphologies, *Journal of Colloid and Interface Science* (2013), doi: http://dx.doi.org/10.1016/j.jcis.2013.10.046

Synthesis of selenium particles with various morphologies

Ajeet Kumar, Igor Sevonkaev, and Dan V. Goia*

Clarkson University, Potsdam, NY 13699-5814, USA

Tel.: 1-315-268-4411; Fax: 1-315-268-2139; e-mail: goiadanv@clarkson.edu

Abstract

Uniform selenium spherical particles were prepared by reducing selenous acid with hydroquinone in the presence of Daxad 11G. The red colored colloidal dispersions displayed a distinct plasmon band at ~612 nm and were stable for extended time due to the negative surface potential of the particles. Structural analyses indicated that the Se spheres were aggregates of nanosize subunits crystallized in the hexagonal system. Selenium wires and rods were obtained by changing the pH and the composition of the precipitated dispersions and incubating them for extended time at moderate temperatures. The addition of a co-solvent played a major role in the re-crystallization of selenium spheres into anisotropic structures.

Key words: Selenium spheres; hydroquinone; Daxad 11G; colloidal dispersion, recrystallization

1. Introduction

The excellent photoconductivity and enhanced piezoelectric, thermoelectric, and non-linear responses of selenium are routinely exploited in many applications including solar cells, rectifiers, photographic exposure meters, photocells, pressure sensors, and xerography.[1, 2] The range of applications can be further broadened when the element is available in dispersed form.[3] For example, selenium nanoparticles paired with suitable bio-degradable stabilizers are often used in the bio-medical field.[4] For these reasons, the study of selenium particles has gained lately considerable importance and significant efforts are directed toward their synthesis, characterization, and modification. Dispersed selenium with various crystalline structures has been obtained in a wide variety and shapes including nanowires,[5] nanoribbons,[6] nanoplates,[7] nanotubes,[8] and spheres.[2] Byron *et al.*[9] were the first to synthesize trigonal Se nanowires using a solution precipitation process. Johnson *et al.*[1] synthesized both amorphous and monoclinic selenium in reverse micelles. Amorphous selenium (a-Se) with a mean particle size of 2 nm was also prepared in aqueous solution by Dimitrijevic *et al.*[10] Such dispersions, however, were subject to strong photo-degradation and thus unstable. Quintana *et al.*[11] used pulsed laser ablation to prepare amorphous selenium particles and deposited them on various substrates (Au, Si, glass). Trigonal selenium (t-Se) particles have also been produced by adsorption through vapor phase diffusion,[12] confinement in zeolite pores or cancrinite nanochannels,[13] and crystallization of amorphous selenium melt.[14] The majority of these processes yield stable selenium dispersions only at low concentrations and are not suitable for large-scale manufacturing. For this reason, the development of many practical applications involving dispersed selenium particles has been slow or put on hold. This paper describes a simple, volumetrically efficient, and easily scalable precipitation method for producing monodisperse selenium particles in either dried form or as stable dispersions. The process

consists of reducing selenous acid with hydroquinone in the presence of a dispersing agent (Daxad 11G) and includes several novel elements. First, we show for the first time that hydroquinone can be used effectively for the preparation of dispersed elemental selenium. Secondly, the method generates stable dispersions of uniform selenium particles at significantly higher concentrations than previously demonstrated. Finally, it is being shown that the precipitated uniform selenium spheres can be subsequently converted into anisotropic particles.

2. Experimental

2.1. Materials

Selenous acid (H_2SeO_3, 97%) and hydroquinone ($C_6H_6O_2$, 99%) were obtained from Alfa Aesar (Massachusetts, USA). Daxad11G (sodium salt of naphthalene sulfonate formaldehyde condensate) was purchased from Fluka (Missouri, USA). All reagents were used without further purification. All glassware was thoroughly cleaned before the experiments. Deionized water (DI) was used in the preparation of all solutions.

2.2. Preparation of selenium spheres

The reacting solutions of selenous acid (100 cm^3, 1.4 $mol.dm^{-3}$) and hydroquinone (50 cm^3, 2.2 $mol.dm^{-3}$) were prepared by dissolving the respective compounds in deionized water. The dispersant (2.2 g Daxad 11G) was dissolved in the latter. After maintaining the solutions at 65 °C for 10 min, the selenous acid was added quickly to the stirred hydroquinone/Daxad 11G solution. While holding the temperature at 65 °C, the stirring was continued for 30 more minutes to ensure the complete reduction of selenium and the formation of a stable colloidal dispersion. For structural characterization, the particles were separated by centrifugation, washed three times with DI water and dried for 4 hours at 40 °C.

2.3. Characterization

The size and morphology of selenium particles were assessed by transmission electron microscopy (TEM) and field emission scanning electron microscopy (FESEM). The size distribution of the particles was determined from the electron micrographs using ImageJ software. Their degree of dispersion was assessed by comparing the SEM size and the average particle size determined by dynamic light scattering (DLS) analysis. The optical properties of selenium particles were monitored as a function of time with a Perkin–Elmer Lambda 35 UV–Vis Spectrophotometer. Small dispersion aliquots (1.0 cm^3) removed from the reaction vessel were first diluted in a 50 cm^3 volumetric flask and then transferred in the 10-mm-optical-path-length quartz cuvette. The scanning range used was from 400 nm to 900 nm and the scanning speed was 960 nm/min. The surface charge of Se particles was measured with a ZetaPals instrument (Brookheaven Instruments). The structure of particles was investigated by X-ray diffraction (XRD) using a Bruker D8 instrument. For the diffraction pattern acquisition, the step width and period were 0.02° and 1.5 s respectively, while the source, sample, and detector slits were 2, 0.6, and 1 mm. The Scherrer equation was used to calculate the size of the constituent crystallites.

3. Results and Discussion

3.1. Precipitation of selenium spheres

The emergence of a red-brick color only 1-2 min after mixing the reactant solutions was a clear indication that hydroquinone reduces easily selenous ions to elemental selenium. The efficacy of the reductant was further demonstrated by the quantitative precipitation of selenium in less than 30 min. The facile transfer of electrons from the reductant molecules to the selenous ions is not

surprising considering that the redox potential for the overall redox reaction (Eq. 1) is positive and quite large (E^0 = + 0.69 V).

$$H_2SeO_3 + 2\,C_6H_6O_2 \rightarrow Se + 2\,C_6H_4O_2 + 3\,H_2O \qquad \text{(Eq. 1)}$$

Both FESEM and TEM analyses revealed that the isolated solids consisted of uniform spherical particles **(Fig.1)**. Their average size determined by image analysis was 210 ± 20 nm.

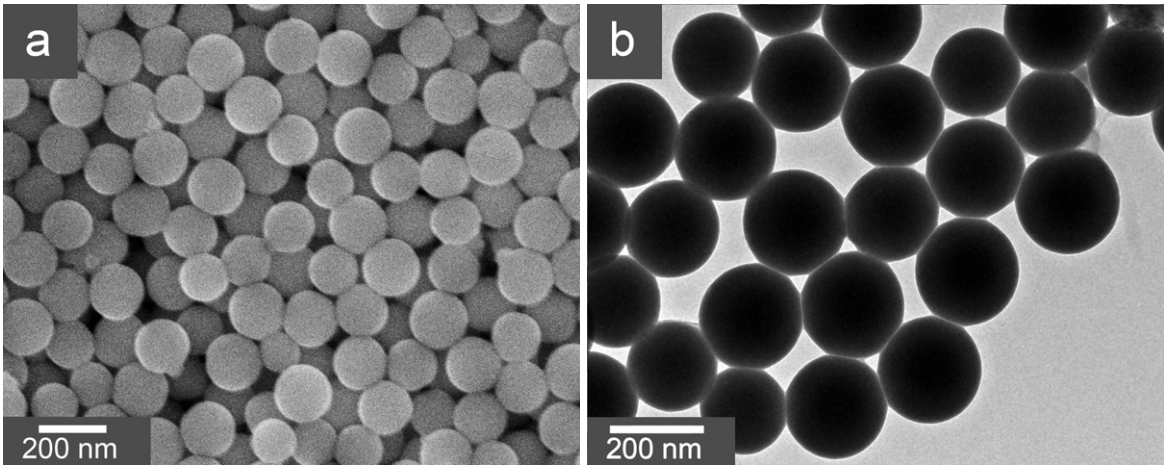

Fig.1. FESEM (a) and TEM (b) images of selenium particles formed in the experimental conditions given in section 2.2.

The fact that the particle size distribution measurements by DLS (**Fig. 2a**) yielded a similar value (215 nm) was a proof that the spheres were non-aggregated entities. This was further confirmed by the good dispersion stability and the presence of a plasmon band at 612 nm (**Fig. 2b**). The high negative surface potential of Se spheres (–51.0 mV), measured by the same DLS technique, was is likely responsible for both absence of particle aggregation and dispersion stability.

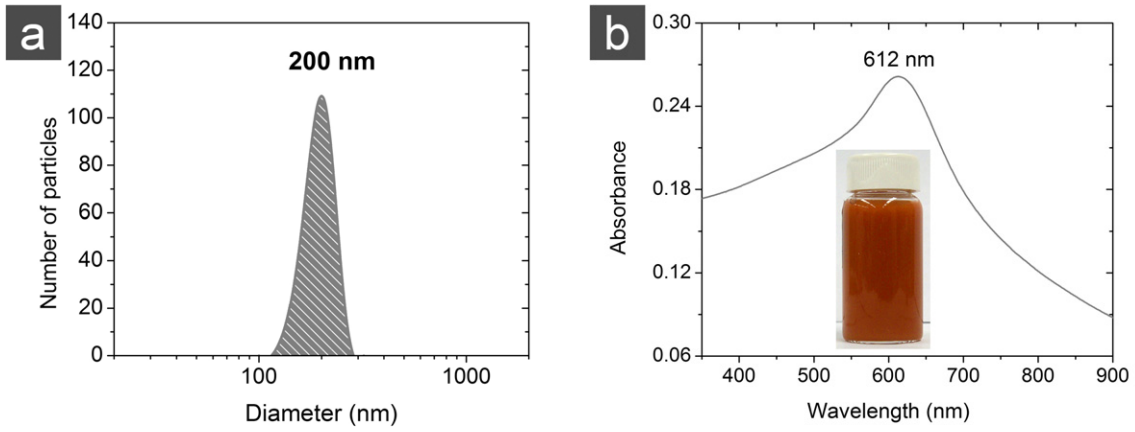

Fig. 2. a) Particle size distribution of Se particles shown in Figure 1; b) UV-Vis spectrum and photo (insert) of the selenium dispersion prepared in the conditions given in section 2.2

The composition and crystalline structure of dried solids were investigated by EDX and XRD respectively. The former technique confirmed that selenium was the major component and detected only traces of carbon, likely from the residual dispersing agent (**Fig. 3a**). The XRD pattern of the sample is presented in **Fig. 3b**. All diffraction peaks match the 2θ angles listed for a hexagonal selenium phase (JCPDS File 006-0362) as well as the expected ratio of peak intensities.

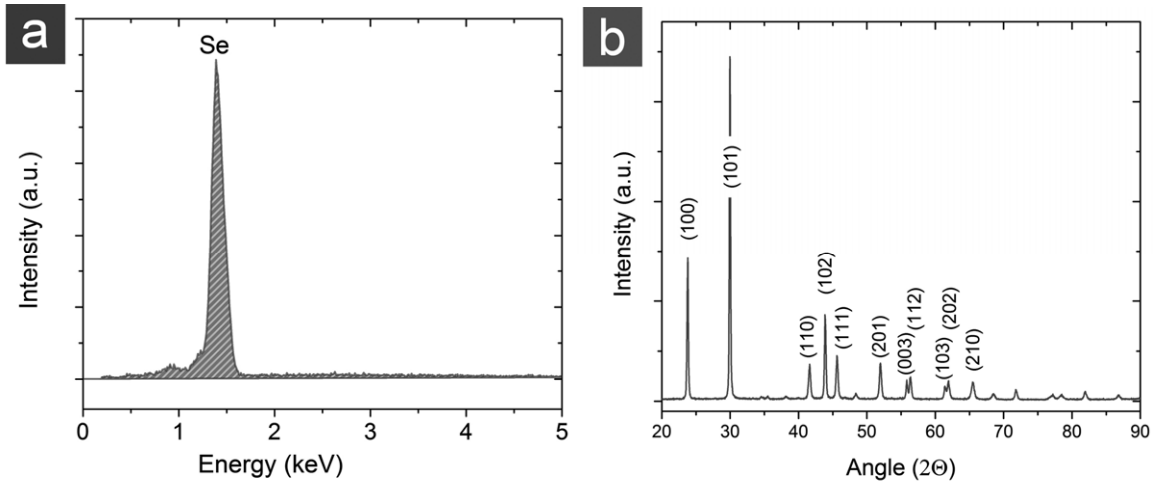

Fig. 3. a) EDX and b) X-ray diffraction patterns of selenium particles shown in **Fig. 1**

The average crystallite size obtained by applying the Scherrer's method to the {100} and {101} reflections was ~40 nm. The discrepancy between this value and the diameter of the spheres suggests that the latter were formed by an aggregation process involving smaller crystalline precursor subunits. This mechanism, typical for the precipitation of spherical particles in homogeneous solutions, was extensively investigated and documented experimentally [15-17] and theoretically [18-22] for precipitated Ag, Au, and CdS.

A surprising finding of this study was the lack of correlation between the crystalline structure identified by XRD and the known optical properties of selenium. According to most sources,[9, 23, 24] elemental selenium exists in five common allotropic forms: amorphous red, three monoclinic red polymorphs (α, β, and γ), and gray hexagonal. However, both the Se dispersion and the isolated dried particles prepared in this study displayed a red-brick color (Fig. 2 inset) despite having a hexagonal crystal lattice. A plausible reason for this inconsistency is that the size and not the crystalline structure dictates its optical properties. Indeed, other elements (Au, Ag) display vivid colors and a distinct plasmon band only if they have nanosize dimensions *and* are well dispersed.[25-27] While the size of selenium spheres (> 200 nm) is too large to give rise to a plasmon band in the visible range, the constituent nanosize crystallites have the right dimensions to display plasmonic properties.[2, 28-30] Considering the aggregation mechanism involved in the formation of spheres, it is inevitable that some dispersant and reaction byproduct (1,4-benzoquinone) are trapped in the internal grain boundary. The non-metallic phase prevents the electron 'hopping' between crystallites and allow them to behave as ‘stand-alone’ resonators when interacting with electromagnetic radiation. The presence of a non-metallic component in the internal grain boundary was confirmed during transmission electron microscopy investigations (**Fig. 4**). After exposing the selenium spheres to the high energy electron beam for a short time, the constituent selenium crystallites sintered forming a compact core.

Concomitantly, the organic matter migrated from the internal grain boundary to the periphery of the particle (semitransparent shell in **Fig. 4b**).

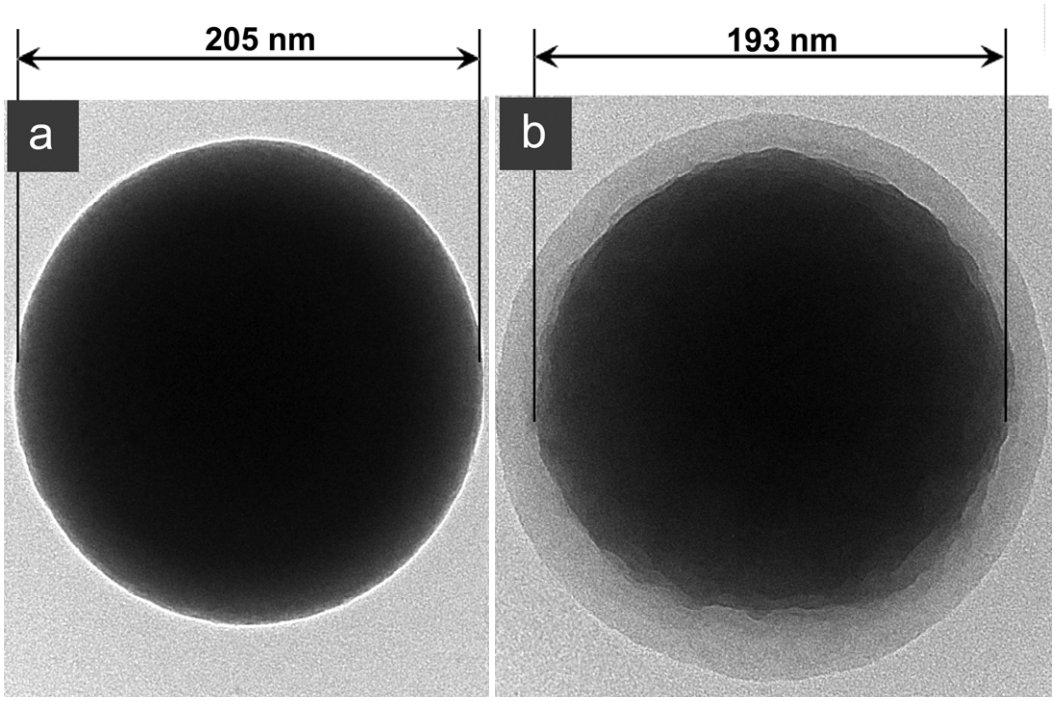

Fig. 4. TEM images of a) a selenium sphere as precipitated and b) same particle after exposure to a high energy electron beam

Taking in consideration the diameter of the original particle (205 nm) and the size (193 nm) of the sintered Se core (**Fig. 4b**), simple calculations indicate that the dispersant trapped represents ~20% of the precipitated sphere volume (or ~4% of the weight if the specific gravities of the two phases are considered). This volume is sufficient to provide the necessary separation between the constituent crystallites so that they can display plasmonic properties responsible for the red color.

3.2. Formation of anisotropic selenium structures

The size, shape, and color of precipitated selenium spheres were not affected even if the dispersions were left standing for several weeks. Altering the pH and the composition of the dispersions, however, brought significant changes in these properties. When the pH at the end of

the precipitation was adjusted to 12.0 with NaOH and the particles were incubated at 40 °C, the dispersion was quickly destabilized and the color of the particles changed from brick red to grayish black. The SEM images taken after 16 h incubation revealed the presence of large Se crystals shaped as hexagonal prisms with a thickness of ~1.0 μm and a length of ~2.0 μm (**Fig. 5a**). When 20% of ethanol (by volume) was added to the dispersion after the pH adjustment, the size and morphology of the particles evolved differently. After incubation for 16 h at 40 °C they still had rod-like morphology and a similar length but were thinner (200–300 nm) and aggregated in "flower-like" assemblies (**Fig. 5b**)

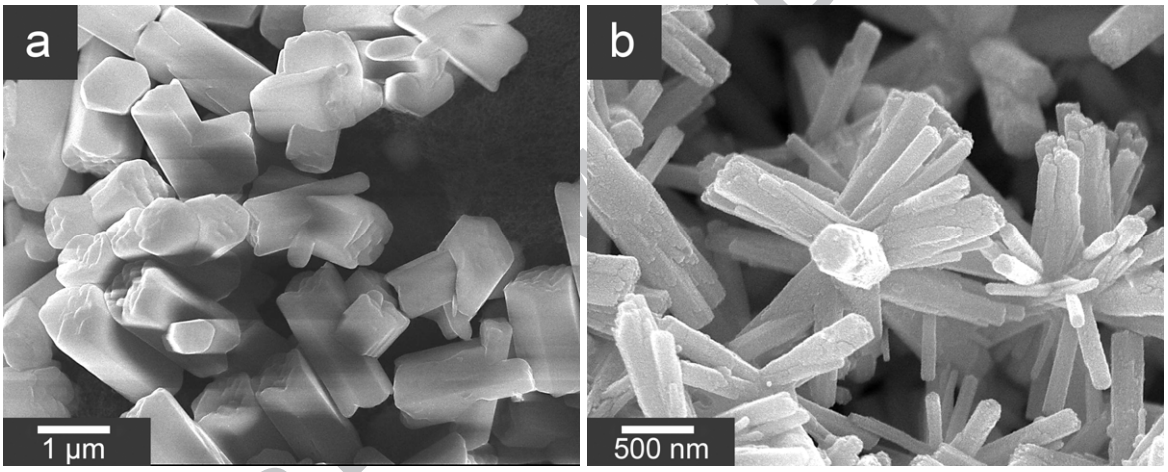

Fig. 5. a) Hexagonal prisms formed by incubating for 16 hours at 40 °C a dispersion of Se spheres adjusted to pH 12.0; b) "flower-like" aggregates of selenium rods formed in the presence of ethanol

When a second solvent was present, the conversion from spheres to anisometric structures occurred even without pH adjustment. When 20 cm^3 of selenium dispersion was vigorously mixed with 10 mL cyclohexane and left standing at 40 °C for 24 h, the red selenium particles migrated to the interface between the two immiscible liquids and their color slowly changed to gray. During the incubation, the shape of the selenium particles gradually changed from spherical to needle-like. The evolution of particle morphology as a function of time is

shown in **Fig. 6**. The uniform spherical particles start to lose their integrity after only 1 h as relatively low aspect ratio anisotropic structures (rods, platelets) start to form (**Fig. 6a**). After 12 hours, aggregates of higher aspect ratio wires emerging from a few growth centers were detected (**Fig. 6b**). Their average length and thickness was 2-4 μm and respectively 200–300 nm. After 24 hours, the length if the wires increased and they were freed from the "flower-like" aggregates (**Fig. 6c**). The evolution of particle size and shape was dramatically different when the dispersion was sonicated for 10 minutes before incubation. In this case, at the end of the 24 h period the particles consisted mostly of low aspect ratio ellipsoids along with few short (1–2 μm) wires. It is noteworthy that the sonication had a significant impact only on the aspect ratio of the particles, the short ellipsoids having roughly the same diameter as the long wires formed in the non-sonicated sample (**Fig. 6d**).

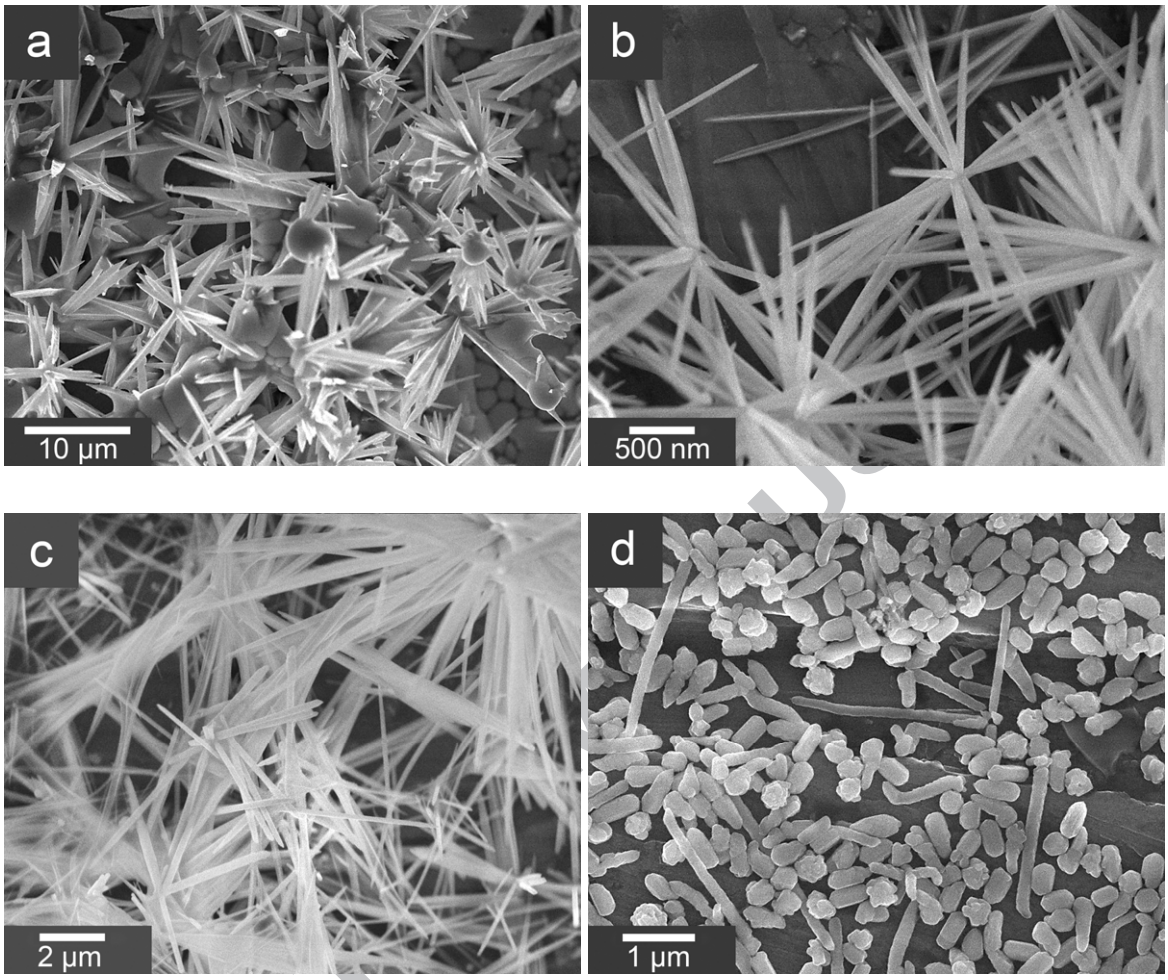

Fig. 6. FESEM images of selenium particles recrystallized at the water/cyclohexane interface after incubating a non-sonicated dispersion at a) 40 °C for 1 h, (b) for 12h, (c) for 24 h; (d) Se particles incubated for 24 h after 10 min sonication

The observed changes in the size, morphology, and color of the selenium particles are the result of the re-crystallization of original spheres. In order for this process to proceed at a considerable rate, the conditions ensuring the stability of the spheres need to be changed. It is well known that selenium is more soluble at high temperature and elevated pH.[31] In these conditions, the dissolution of spheres and re-deposition of selenium atoms needed for the growth of the large crystalline entities observed is accelerated. Based on the rapid change in the color of

the dispersions, it appears that the mass transport occurs first inside each sphere causing the growth of the internal crystallites to dimensions above the threshold value that triggers plasmonic properties. This 'intra-sphere' transport of atoms is facilitated by the diffusion of Daxad 11G from the internal grain boundaries into the dispersion medium as a result of its increased solubility at high pH due to the deprotonation of sulfonic groups. As previously shown [32[, the properties of this compound (including solubility) differ markedly when the pH is changed from acidic (!1.0 for the precipitated dispersion) to 12.0. The 'inter-spheres' mass transport leading to the selenium re-crystallization into large anisotropic entitles is facilitated by the contact points between particles in the aggregates formed after dispersion destabilization. In the early stages, these aggregates re-crystallize into compact large irregular selenium entities that act simultaneously as reservoirs of selenium atoms and 'centers' for the growth of long wires (**Fig. 6a,b**). Once the supply of atoms in these 'growth centers' is exhausted, the wires are freed forming 'stand alone' structures (**Fig. 6c**). The energy provided by sonication causes the formation of a larger number of smaller aggregates/'growth centers'. This reduces the size of selenium atoms reservoirs available for growth and leads to the formation of short ellipsoids.

4. Conclusions

A simple method for preparing stable concentrated aqueous dispersions of uniform selenium spheres is described. The red colored particles are formed by the aggregation of smaller selenium subunits crystallized in the hexagonal system. The separation of nanosize internal subunits by a layer of dispersant incorporated in the internal grain boundary is responsible for the uncharacteristic red color for the hexagonal lattice. The selenium spheres can be slowly converted into anisotropic particles of various sizes and shapes by changing the pH and the composition of the dispersions. A mechanism for the recrystallization is proposed. The simplicity

of the precipitation process, the high concentration of selenium in the prepared dispersions, and the ability to control the size and shape of the final particles makes the described process a viable route for large scale preparation of selenium particles for practical applications.

References

[1] J.A. Johnson, M.L. Saboungi, P. Thiyagarajan, R. Csencsits, D. Meisel, J. Phys. Chem. B 103 (1999) 59.

[2] C.P. Shah, M. Kumar, P.N. Bajaj, Nanotechnology 18 (2007).

[3] D.H. Qin, J.W. Zhou, C. Luo, Y.S. Liu, L.L. Han, Y. Cao, Nanotechnology 17 (2006) 674.

[4] M.A. Bakir, G. Alya, A. Mohammad, R. Azroony, F. Kasies, J. Radioanal. Nucl. Chem. 266 (2005) 165.

[5] B. Zhang, X.C. Ye, W. Dai, W.Y. Hou, F. Zuo, Y. Xie, Nanotechnology 17 (2006) 385.

[6] X.B. Cao, Y. Xie, S.Y. Zhang, F.Q. Li, Adv Mater 16 (2004) 649.

[7] H.Y. Yin, Z. Xu, H.H. Bao, J.Y. Bai, Y.F. Zheng, Chem. Lett. 34 (2005) 122.

[8] H. Zhang, D.R. Yang, Y.J. Ji, X.Y. Ma, J. Xu, D.L. Que, J. Phys. Chem. B 108 (2004) 1179.

[9] B. Gates, Y. Yin, Y. Xia, J. Am. Chem. Soc. 122 (2000) 12582.

[10] N.M. Dimitrijevic, P.V. Kamat, Langmuir 4 (1988) 782.

[11] M. Quintana, E. Haro-Poniatowski, J. Morales, N. Batina, Appl. Surf. Sci. 195 (2002) 175.

[12] Z.K. Tang, M.M.T. Loy, T. Goto, J. Chen, R. Xu, Solid State Commun. 101 (1997) 333.

[13] A.V. Kolobov, H. Oyanagi, V.V. Poborchii, K. Tanaka, Phys Rev B 59 (1999) 9035.

[14] H.Y. Zhang, Z.Q. Hu, K. Lu, Nanostruct Mater 5 (1995) 41.

[15] B.J. Morrow, E. Matijevic, D.V. Goia, J. Colloid Interface Sci. 335 (2009) 62.

[16] L. Suber, I. Sondi, E. Matijevic, D.V. Goia, J. Colloid Interface Sci. 288 (2005) 489.

[17] S. Libert, V. Gorshkov, V. Privman, D. Goia, E. Matijevic, Adv. Colloid Interface Sci. 100 (2003) 169.

[18] S. Libert, V. Gorshkov, D. Goia, E. Matijević, V. Privman, Langmuir 19 (2003) 10679.

[19] J. Park, V. Privman, E. Matijević, J. Phys. Chem. B 105 (2001) 11630.

[20] V. Privman, Ann. N. Y. Acad. Sci. 1161 (2009) 508.

[21] V. Privman, D.V. Goia, J. Park, E. Matijević, J. Colloid Interface Sci. 213 (1999) 36.

[22] D.T. Robb, I. Halaciuga, V. Privman, D.V. Goia, J. Chem. Phys. 129 (2008) 184705.

[23] U.K. Gautam, M. Nath, C.N.R. Rao, J. Mater. Chem. 13 (2003) 2845.

[24] N.N. Greenwood, Chemistry of the elements. Butterworth-Heinemann, Oxford [u.a., 1997.

[25] Z.H. Lin, C.R.C. Wang, Mater. Chem. Phys. 92 (2005) 591.

[26] K. Balantrapu, D.V. Goia, J. Mater. Res. 24 (2009) 2828.

[27] I. Halaciuga, D.V. Goia, J. Mater. Res. 23 (2008) 1776.

[28] C. Dwivedi, C.P. Shah, K. Singh, M. Kumar, P.N. Bajaj, Journal of Nanotechnology 2011 (2011) 1.

[29] S. Dwivedi, A.A. Alkhedhairy, M. Ahamed, J. Musarrat, PLoS One 8 (2013) e57404.

[30] S.Y. Zhang, J. Zhang, H.Y. Wang, H.Y. Chen, Mater. Lett. 58 (2004) 2590.

[31] V.S. Minaev, S.P. Timoshenkov, V.V. Kalugin, J Optoelectron Adv M 7 (2005) 1717.

[32] L. Lu, D.V. Goia, J. Colloid Interface Sci. 407 (2013) 122.

Research highlights

- Stable aqueous dispersions of uniform selenium spheres were prepared
- The selenium spheres are formed by the aggregation of nanosize subunits
- The subunits are responsible for the optical properties of selenium particles
- The spheres can be converted into anisotropic structures by recrystallization
- The pH and presence of a co-solvent have a major effect on the recrystallization process

Graphical Abstract

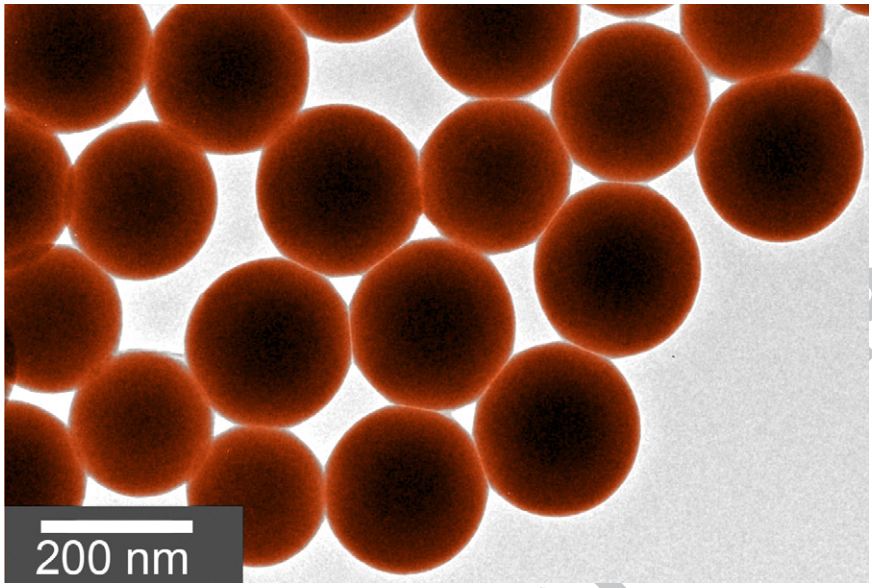

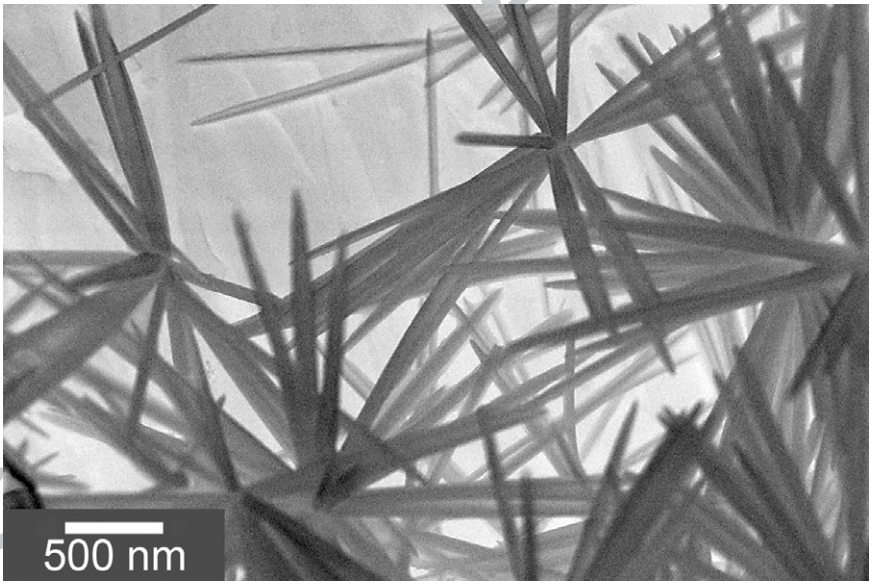

Stable dispersions of uniform selenium spherical particles were prepared by reducing selenous acid with hydroquinone in presence of Daxad 11G as dispersant. Anisotropic structures where obtained by incubating the dispersions at high pH or in the presence of a co-solvent.